Int. J. Multiphase Flow, Vol. 3, pp. 517–532. Pergamon/Elsevier, 1977. Printed in Great Britain

BEHAVIOUR OF LIQUID FILMS AND FLOODING IN COUNTER-CURRENT TWO-PHASE FLOW—PART 1. FLOW IN CIRCULAR TUBES

S. SUZUKI* and T. UEDA

Department of Mechanical Engineering, University of Tokyo, Bunkyo-Ku, Tokyo 113, Japan

(*Received* 6 *April* 1977; *received for publication* 14 *June* 1977)

Abstract—Experimental results are presented on the flooding gas velocity in tubes over a wide range of parameters—tube diameter, tube length, liquid flow rate, liquid viscosity and surface tension. The flooding phenomenon is caused by interaction between the waves on the liquid film and the upward gas stream. By measuring variation of the maximum height of the wavy liquid films with an increase of the gas flow rate, the complicated effects of tube length and surface tension on flooding are revealed. The data of the flooding velocity are empirically correlated in terms of nondimensional groups for each tube length.

1. INTRODUCTION

Counter-current two-phase flow in which liquid flows down on the inner surface of a tube and gas flows upwards through the core is often encountered in industrial systems, and it is noted that behaviour of the liquid films in the flow is complicated. The flooding phenomenon, the transition of part of liquid to a climbing film on increasing gas velocity, has attracted attention of many researchers in connection with the performance of chemical plants such as wetted wall columns and packed towers and lately with the safety of nuclear reactors. Many experimental studies have been carried out on the flooding condition. Nevertheless the mechanism of flooding is still uncertain and meaningful experiments which provide insight into the mechanism are limited.

A comprehensive experiment was performed by Kamei *et al.* (1954) in which the tube diameters were varied from 19 to 49 mm in a 2.5 m tube length. In their report, the ratio of the gas flow rate G_G and the liquid flow rate G_L at the onset of flooding was given by the following equation in a form of nondimensional representation,

$$\left(\frac{G_G}{G_L}\right) = 198\left(\frac{4G_L}{\pi D_i \mu_L}\right)^{-1.225}\left(\frac{\sigma}{D_i^2 \rho_L g}\right)^{-0.23}\left(\frac{\mu_G}{\mu_L}\right)^{0.71}\left(\frac{\rho_G}{\rho_L}\right)^{0.13}\left(\frac{D_i^3 \rho_L{}^2 g}{\mu_L{}^2}\right)^{0.231} \quad [1]$$

where, μ_L and μ_G, and ρ_L and ρ_G are the viscosities and densities of the liquid and gas phases respectively, and D_i denotes the tube diameter and σ the surface tension. Wallis (1961) derived the following nondimensional variables including the superficial velocities of the gas and liquid phases U_G and U_L respectively,

$$U_G^* = U_G \rho_G{}^{1/2}[gD_i(\rho_L - \rho_G)]^{-1/2}, \quad [2]$$

$$U_L^* = U_L \rho_L{}^{1/2}[gD_i(\rho_L - \rho_G)]^{-1/2} \quad [3]$$

and suggested a simple equation for the flooding transition of air–water systems as follows:

$$\sqrt{U_G^*} + \sqrt{U_L^*} = C \quad [4]$$

where the value of C depends on the conditions of inlet and outlet of the liquid phase. In the above equation the effects of viscosity and surface tension are not included. Wallis (1962) and

*Present Address: Unicellex Development Division, Unitika Ltd., 23-Kozakura, Uji-City, Kyoto 611, Japan.

Clift *et al.* (1966) carried out the experiments on high viscous liquids and showed that the gas velocity required to cause flooding was reduced with increasing liquid viscosity under a constant liquid flow rate. For viscous liquids Wallis (1969) obtained a new correlation of the form

$$\sqrt{U_G^*} + a\sqrt{U_L^*} = C \qquad [5]$$

where a and C are constants for a given liquid but vary with the viscosity.

It was pointed out by Hewitt *et al.* (1965, 1970) that tube length has a very important effect on flooding. The investigation made by Hewitt *et al.* (1965, 1970) in a 31.8 mm tube diameter covered the tube lengths ranged from 0.23 to 3.66 m and the pressures from 1.0×10^5 to 2.75×10^5 N/m^2, and showed that the gas velocity for flooding decreased with increasing tube length and pressure. There are few reports about the effect of surface tension on flooding. The experimental results of Kamei *et al.* (1954) suggested a trend of the flooding gas velocity increasing with a decrease of surface tension and that of Shires & Pickering (1965) showed the opposite trend.

It has been considered that the flooding phenomenon is brought about by interaction of the waves on the film and the gas stream. Hewitt *et al.* (1965) have observed that the amplitude of waves on the liquid film increases progressively as the gas velocity is increased. Theoretical studies on the mechanism of flooding have been made by Shearer & Davidson (1965), Getinbudakler & Jameson (1969) and Kusuda & Imura (1974). In these theories, the flooding transition is postulated as a phenomenon associated with the interfacial wave instability, which takes place when the gas velocity reaches a critical value and causes an abrupt increase in wave amplitude. For instance, Kusuda & Imura applied the Kelvin–Helmholtz instability theory for inviscid fluids to the counter-current two-phase flow, and derived the critical slip velocity between the gas and liquid phases at which interfacial waves become unstable, as

$$u_G + u_L = (2\pi\sigma/\lambda\rho_G)^{1/2} \qquad [6]$$

where u_G and u_L are mean velocities of the upward gas stream and the downward liquid film flow, respectively. Supposing the flooding condition is given by the above equation, they derived the flooding velocity by assuming that the wave length λ is directly proportional to the mean film thickness. However, neither of the above theories includes the effects of tube diameter and tube length which are practically of considerable importance.

In this report, behaviour of the liquid films is examined and experimental results are presented on the flooding velocity, the gas velocity at the onset of flooding, over a wide range of parameters. Observation by a high speed camera and measurements by a contact probe method are made of the growth of waves on the liquid film with an increase of the gas rate. From the data obtained the effects of such parameters as tube diameter and surface tension on flooding are discussed. As for the flooding condition, empirical equations are proposed for each tube length.

2. EXPERIMENTAL APPARATUS AND PROCEDURE

A schematic diagram of the experimental apparatus is shown in figure 1. The test tube is made of transparent acrylic resin. The air introduced from the bell-shaped section passes through a test tube and an upper tube. Air flow is metered with a rotameter or an orifice flow meter and is delivered to the atmosphere by a turbo-blower. On the other hand, the liquid pumped up from a storage tank is introduced into the liquid inlet section through rotameters. The liquid passed through a porous sinter section flows down on the inner surface of the test tube in a state of a film. Below the flooding point, all the liquid flows downwards and falls from the bell-shaped section to a drain receiver. Above the flooding point, on the other hand, part of the liquid flows downwards and the remainder

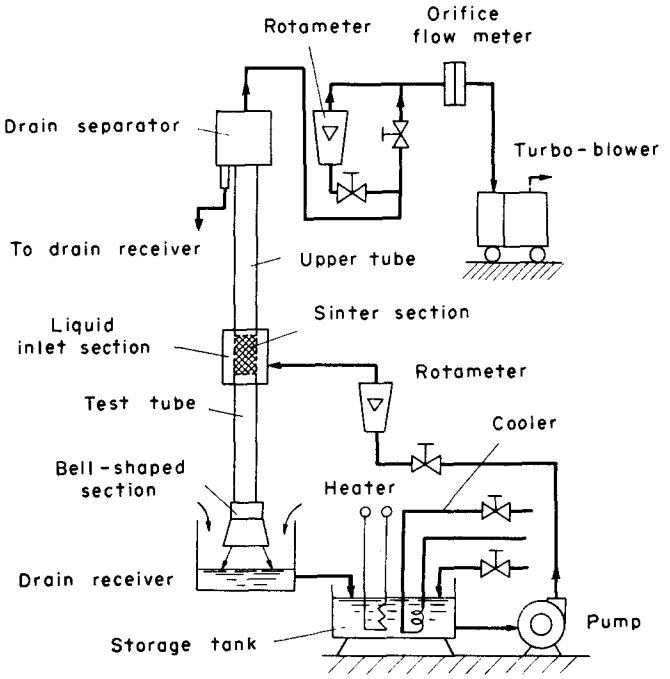

Figure 1. Schematic diagram of experimental apparatus.

of the liquid flows upwards to the drain separator. The separated liquid comes back to the storage tank through the drain receiver. During the experiment the liquid temperatures were adjusted to 25 ± 1°C for water and aqueous sec.-octyl alcohol solutions and 35 ± 1°C for aqueous glycerol solutions.

The flooding gas rate was determined in this experiment by increasing gas flow rate in a small increment under a constant liquid flowrate. Measurements of the flooding velocity were carried out in a range of parameters as summarized in table 1. The diameters of the test tubes were 10, 18 and 28.8 mm I.D. By using water, aqueous glycerol solutions and aqueous sec.-octyl alcohol solutions as the test liquids, liquid viscosity and surface tension were varied from 9.0×10^{-4} to 2.4×10^{-2} Nsec/m^2 and from 6.8×10^{-2} to 3.7×10^{-2} N/m, respectively. The surface tensions shown in table 1 are the values measured in a equilibrium state. The dynamic surface tension of sec.-octyl alcohol solutions has been measured by Addison (1944, 1945), which results show that the freshly formed surface of the solutions attains its equilibrium state in a short time.

Observation of the state of wavy liquid surface and the process of flooding was performed by taking axial view photographs with a high speed camera installed directly below the bell-shaped section. The test tube used in this observation was 28.8 mm I.D. and 0.59 m long. A contact probe method was used for measuring the maximum height of the liquid film. A movable probe was incorporated in an electric circuit with an audio-oscillator generating a 1000 Hz frequency signal as shown in figure 2. The circuit was so arranged that the fraction of time during which the probe tip contacted with the waves was determined directly from the reading of an electronic counter. The maximum height of the liquid film is defined in this experiment as the distance from the wall surface to a point where the fraction of time is approximately equal to 0.1% of the measured time (10 sec). The test tube used was 28.8 mm I.D. and 1.83 m long, and the measurement was made at seven positions along the test tube with an interval of 0.25 m, i.e. the positions at distances 0.25–1.75 m from the sinter section.

3. BEHAVIOUR OF LIQUID FILMS AND FLOODING PHENOMENON

3.1 *Behaviour of liquid films*

The behaviour of liquid film flow in counter-current two-phase systems is complicated and

Table 1. Experimental conditions for flooding

Tube dia. D_i		10 mm					18 mm					28.8 mm		
μ_L Ns/m^2	σ N/m	Re_L \ L_d m	0.5	1.0	1.5	2.0	Re_L \ L_d m	0.5	1.0	1.5	2.0	Re_L \ L_d m	0.59	1.54	1.83
Water (25°C)															
9.0×10^{-4}	0.068	240-3560	○	○	○	○	390-5240	○	○	○	○	820-8180	○△	○	○
Aqueous glycerol solutions (35°C)															
2.1×10^{-3}	0.056	140-2840	○	○	○	○						320-3620	○		○
5.1×10^{-3}	0.053	30-1030			○							80-1200			○
1.0×10^{-2}	0.053	25-380			○							50-510	○△		○
2.4×10^{-2}	0.053	7-100	○	○	○	○						35-140			○
Aqueous sec.-octyl alcohol solutions (25°C)															
9.0×10^{-4}	0.055	390-3280			○							820-4010			○
9.0×10^{-4}	0.047	390-3930			○							820-8180			○
9.0×10^{-4}	0.037	390-2620			○							820-8180	○△		○

○ Measured conditions
△ Photographic observation

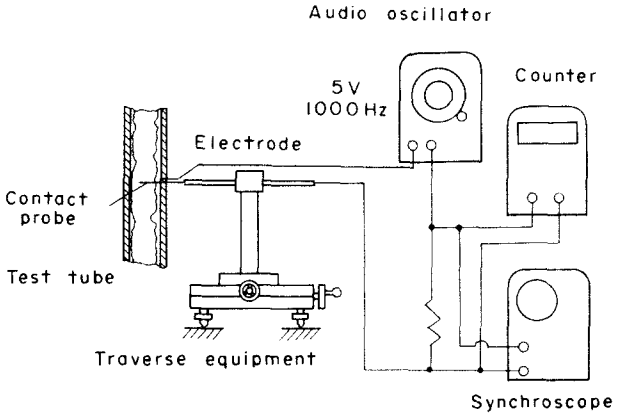

Figure 2. Measurement of maximum liquid film height.

few reports have so far been published about it. Figure 3 shows typical results on the behaviour of liquid films which are plotted on the coordinates of the superficial gas velocity U_G and superficial liquid velocity U_L. If the upward gas velocity U_G is gradually increased in the falling film region, under a constant liquid flow rate Q_L, the waves on the liquid film grow large. These are three-dimensional waves with little deformation in the axial direction. In the course of time, a point is reached at which "a large amplitude wave" is formed on the liquid film somewhere in the test tube and immediately carried upwards by the gas phase. When this wave arrives at the liquid inlet section, the falling film becomes heavily disturbed one and at the same time part of the liquid begins to flow the upper tube in a state of semi-annular flow. The gas velocity at this point is known as the flooding velocity. The large amplitude wave was formed anywhere in the

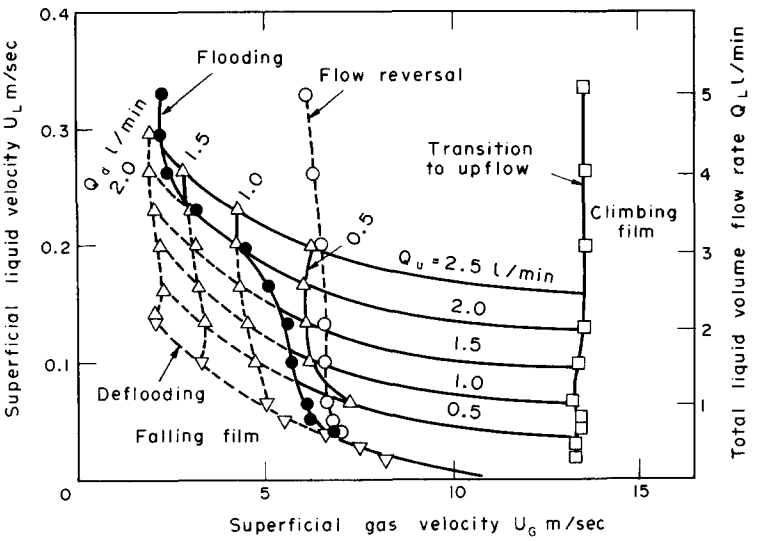

Figure 3. Behaviour of liquid films (water, D_i = 18 mm, L_d = 1.0 m).

test tube in both cases of low liquid flow rates and high viscosities, but showed a trend to be initiated at the positions 20–30 cm upstream of the lower end of the test tube when the liquid flow rate was increased.

The gas velocity is raised over the flooding condition, part of the liquid flows the upper tube as a climbing film and the remainder of the liquid flows the lower test tube as a falling film. Namely a region exists in which both downflow and upflow of liquid are occuring simultaneously. For instance, consider the case where the total liquid flow rate Q_L is 2.0 l/min. When the superficial gas velocity reaches 5.7 m/sec, flooding occurs and then a flow state is realized in which the liquid flow rate of upflow Q_u is 1.3 l/min and that of downflow Q_d 0.7 l/min.

If the upward gas flow rate is further increased, the disturbance of interface of the flow in the test tube decays since the downward liquid flow rate is reduced. The flow regime in the upper tube remains semi-annular flow, but the oscillatory motion of the climbing film becomes weaker with increasing the gas flow rate. With a further increase of the gas flow rate, a point is reached at which all the liquid injected is carried upwards. This point is the transition to upflow.

After all the liquid flows upwards and the wall surface of the test tube is dried up, if the gas rate is gradually reduced now, part of the liquid begins to creep down the test tube from the liquid inlet section. This transition point to downflow is termed the flow reversal point. The gas velocity at this point is far lower than that of the transition to upflow. The liquid flow rate of downflow increases with a reduction of the gas flow rate, and eventually a point is reached at which the upward liquid flow rate becomes zero.

This condition is known as deflooding, where the gas velocity is again far lower than that of flooding. This difference is so-called the hysteresis between flooding and deflooding.

3.2 *Flooding phenomenon*

A typical sequence of frames taken by a high speed camera, figure 4, shows behaviour of the liquid film on flooding. Even at zero gas velocity there are waves on the liquid film but they belong to ripples of small amplitude. These waves become large as the gas flow rate is increased, while they are different in amplitude and length. In many cases a largest one of them is suddenly developed to a large amplitude wave near the lower end of the test tube. Frame (1) shows the state just before the onset of flooding and frame (2) the instant at which such a large wave begins to grow. When the wave height reaches a certain value, the large wave begins to extend toward circumferential direction accompanying with the break up of part of the wave into liquid droplets (3). In the state after the circumferential extension was achieved (4, 5), the

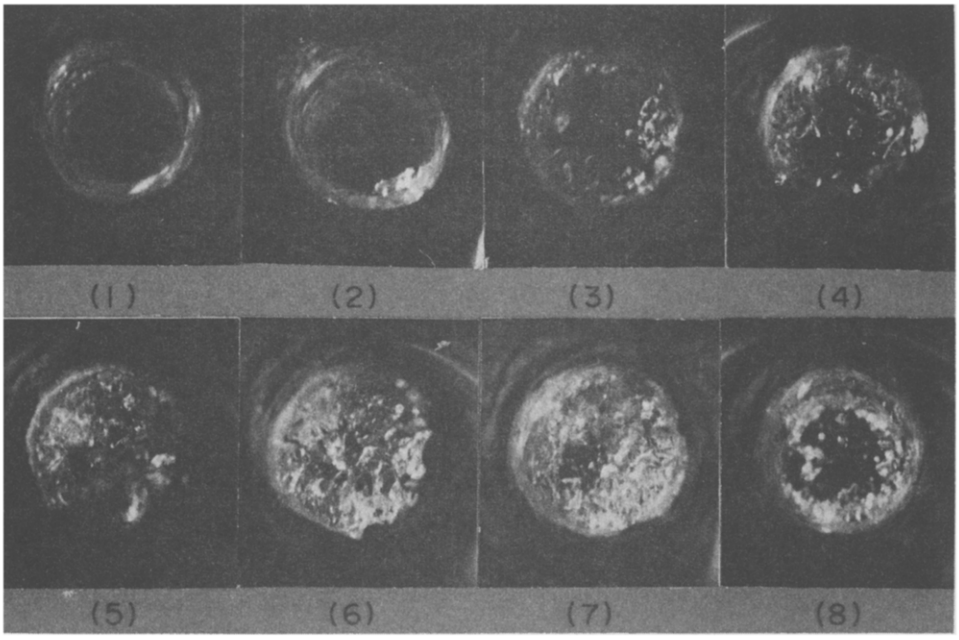

Figure 4. Sequence of frames showing behaviour of the liquid film on flooding (water, frame interval of 40 msec).

liquid appears to occupy most of the tube cross-section (6). Such a large amplitude wave with a number of liquid droplets is then carried upwards by the gas phase (7, 8).

The flooding transition mentioned above takes place in a short time, the time taken from frame (2) to (8) was 0.24 sec. Observation by the high speed camera was also performed for an aqueous glycerol solution and an aqueous sec.-octyl alcohol solution. The aspect of flooding was similar to that of water. Figure 5 shows the wave frequency determined from high speed cine films—the average number of primary waves passing a particular point per second—in the flow state close to flooding. The results suggest that the wave frequency is approximately proportional to the flow rate of liquid phase per unit periphery irrespective of liquid viscosity and surface tension.

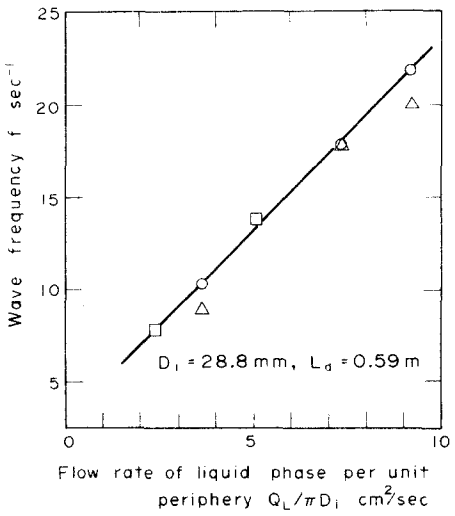

Figure 5. Wave frequency in the flow state close to flooding. ○, Water, $\mu_L = 9.0 \times 10^{-4}$ Nsec/m^2, $\sigma = 0.068$ N/m. △, Aqueous sec.-octyl alcohol solution, $\sigma = 0.037$ N/m. □, Aqueous glycerol solution, $\mu_L = 1.0 \times 10^{-2}$ Nsec/m^2.

4. FLOODING VELOCITY

In this report, the experimental results of the gas velocity at the onset of flooding u_G are plotted against the liquid volume flow rate Q_L or the mean liquid film thickness y_i. Here the value u_G was calculated by the following equation,

$$u_G = G_G \Big/ \left\{ \rho_G \cdot \frac{\pi}{4}(D_i - 2y_i)^2 \right\}$$

where G_G is the gas flow rate at the onset of flooding. For the water–air system, the values of mean liquid film thickness y_i were determined by measuring the hold-up water obtained by a shut-off method for both cases with and without the upward gas stream. Based on the results, the nondimensional mean liquid film thickness $y_i^+ = y_i(g/\nu_L^2)^{1/3}$ was plotted against the liquid film Reynolds number $Re_L = 4\rho_L Q_L/(\mu_L \pi D_i)$ as shown in figure 6, where ν_L is the kinematic viscosity of liquid. This relationship is universal one, therefore, the mean liquid film thickness y_i was derived for the liquid flow rate Q_L by applying the relationship. From this figure it is found that the mean liquid film thickness is approximately independent of the counter-current gas velocities up to the onset of flooding, and is in good agreement with the data obtained for developed falling water films by Ueda & Tanaka (1974) and the calculated values by applying the universal velocity profile to the film flow.

(1) *Liquid flow rate.* The flooding velocity shows a trend to decrease with an increase of the liquid flow rate, as shown in figures 7–11. However, it will be seen from figure 8 that the magnitude of the effect of liquid flow rate changes with the tube length.

(2) *Tube diameter.* Figure 7 shows the results obtained in the case of water films in the tubes of diameters $D_i = 10$, 18 and 28.8 mm. Flooding velocity is elevated with increasing tube diameter. This is the same trend as that obtained by Kamei *et al.* (1954) and Wallis (1961). The flooding velocity shows an approximate trend to increase in proportion to 0.5 power of the tube diameter under a given mean film thickness. According to visual observation, it was clearly confirmed that the wave height in the state just before the flooding becomes higher with increasing the tube diameter.

(3) *Tube length.* Figure 8 shows the results of water films for four tube lengths ranging from 0.5 to 2.0 m in a tube diameter of 10 mm. The flooding velocity decreases with increasing tube length. The effect of tube length on flooding is small in a range of low liquid flow rates but significant in a range of high liquid flow rates. This trend is similar to that obtained by Hewitt *et al.* (1965). However, the effect of tube length is reduced in the case of high viscous liquid, as shown in figure 9.

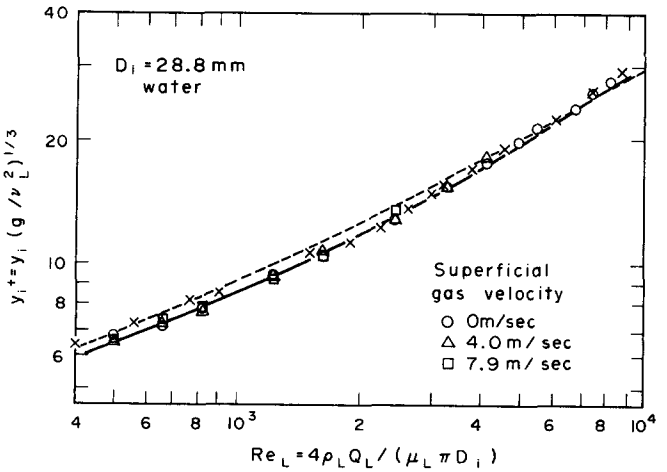

Figure 6. Mean liquid film thickness. ×, Data of Ueda & Tanaka. ----, Calculated by universal velocity profile.

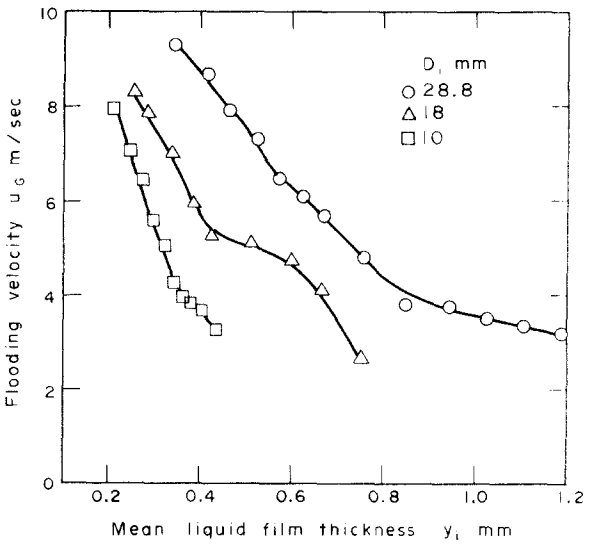

Figure 7. Effect of tube diameter (water, $L_d \doteqdot 1.5$ m).

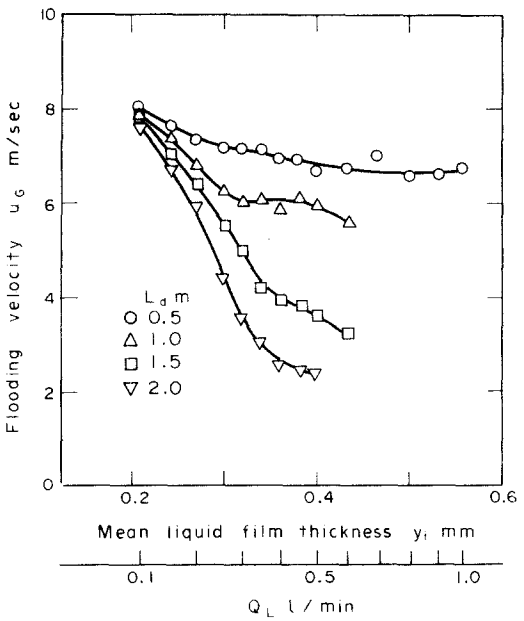

Figure 8. Effect of tube length (water, $D_i = 10$ mm).

(4) *Liquid viscosity.* Figure 10 shows an example of results obtained for five liquid viscosities ranging from 9.0×10^{-4} to 2.4×10^{-2} Nsec/m^2. The flooding velocity has a trend to increase with an increase of the liquid viscosity, but this trend is not so clear in a range of thick film thicknesses.

(5) *Surface tension.* A few studies have been performed on the influence of the surface tension. For changing surface tension, surface active agents are often used, but in this case it is not always easy to know the true surface tension of the dynamic interface. Since aqueous sec.-octyl alcohol solutions are used in this experiment, the characteristics of dynamic surface tension must be examined. According to the measurement of the alcohol solutions by Addison (1945), the equilibrium times of freshly formed surface are about 0.06 and 0.04 sec for solutions of static surface tensions $\sigma = 5.5 \times 10^{-2}$ and 4.7×10^{-2} N/m, respectively. On the other hand, the allowable time for the wave surface is considered to be a reciprocal of the wave frequency (Levich 1962). As the wave frequency in this experimental range is estimated to be 30 sec^{-1} at a

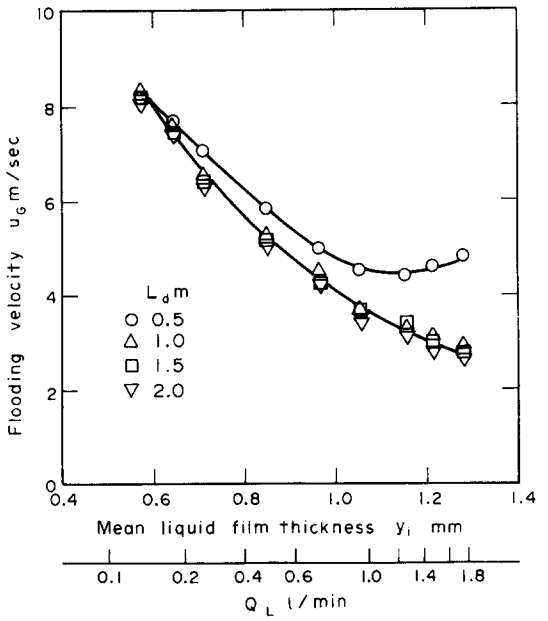

Figure 9. Effect of tube length for high viscous liquids (aqueous glycerol solutions, $D_i = 18$ mm, $\mu_L = 2.42 \times 10^{-2}$ Nsec/m^2).

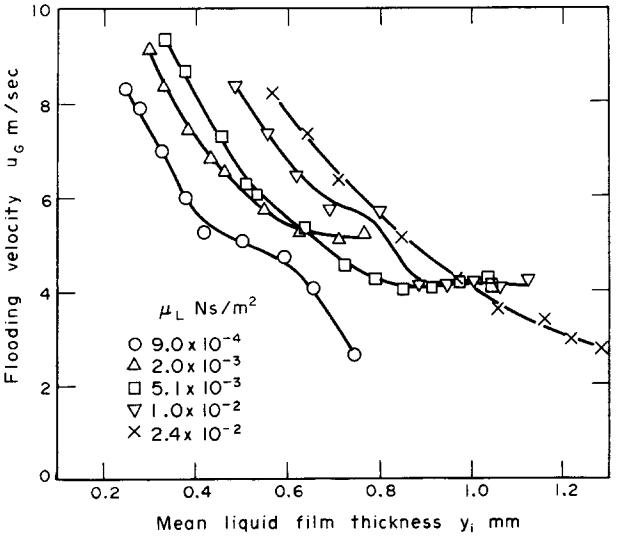

Figure 10. Effect of liquid viscosity ($D_i = 18$ mm, $L_d = 1.5$ m).

maximum from figure 6, the minimum allowable time is about 0.033 sec. Therefore, the maximum dynamic surface tensions corresponding to the test runs of static values $\sigma = 5.5 \times 10^{-2}$ and 4.7×10^{-2} N/m are 5.8×10^{-2} and 4.8×10^{-2} N/m, respectively. These values are slightly higher than the corresponding static values, but this will not reduce so much the reliability of the data in this experiment. For the test run of $\sigma = 3.7 \times 10^{-2}$ N/m, the variation of wave surface tension is negligible because the equilibrium time in this case is shorter than 0.033 sec.

The experimental results which were obtained by changing the surface tension are shown in figure 11. It can be seen from this figure that the effect of surface tension is complicated, and that the flooding velocity takes its maximum value at a condition where the surface tension is close to 5.0×10^{-2} N/m. The contradictory conclusions derived by the experiments of Shires

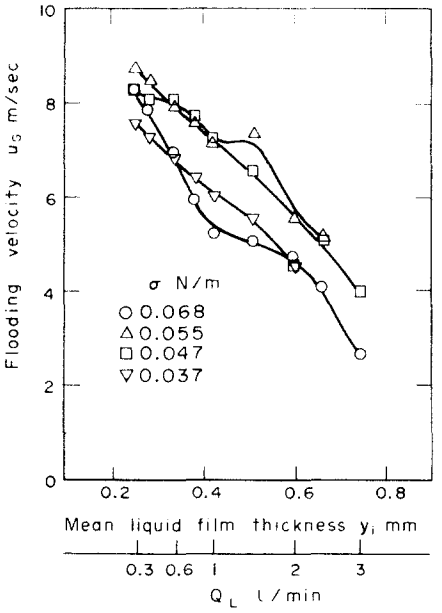

Figure 11. Effect of surface tension (D_i = 18 mm, L_d = 1.5 m).

and Kamei, mentioned before, might be explained by taking into account such a particular effect of surface tension on flooding.

5. MAXIMUM HEIGHT OF LIQUID FILMS

Many experimental results have been reported of waves on falling liquid films in the absence of gas stream (Jones & Whittaker 1966, Isigai *et al.* 1971, Portalski & Clegg 1972). However, the results of those in counter-current two-phase flow are few (Shirotsuka *et al.* 1957, Stainthorp & Batt 1965) and limited in water–air systems. In this experiment, using the test tube having a diameter of 28.8 mm, the maximum height of the wavy liquid films was measured along the test tube in a range of liquid viscosities, surface tensions and gas velocities.

Figure 12 shows the variation of the maximum height of wavy films y_{imax} along the tube in the case without gas stream. The maximum height increases rapidly in a region near the liquid inlet section, but the growth rate is complicated along the tube length as shown by Isigai *et al.* (1971). Whether the waves on the liquid film grow or not in a region below the position about

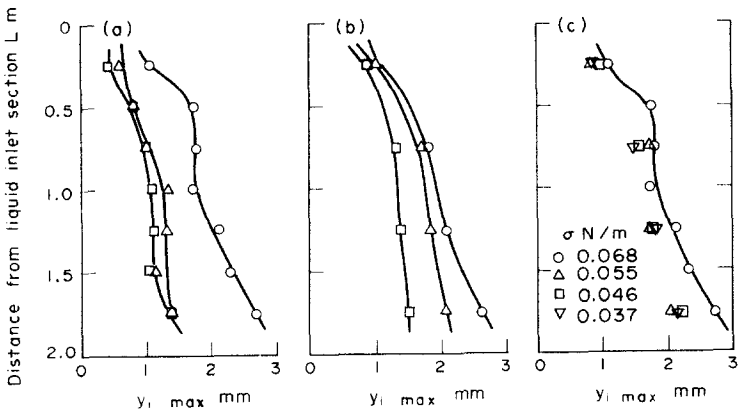

Figure 12. Maximum height of falling liquid film (D_i = 28.8 mm, L_d = 1.83 m, gas vel. u = 0 m/sec). (a) Water, $\mu_L = 9.0 \times 10^{-4}$ Nsec/m^2. ○, Re_L = 4910, y_i = 0.85 mm; △, Re_L = 3270, y_i = 0.67 mm; □, Re_L = 1640, y_i = 0.46 mm. (b) Aqueous glycerol solution, $\mu_L = 5.3 \times 10^{-3}$ Nsec/m^2. ○, Re_L = 664, y_i = 0.94 mm; △, Re_L = 346, y_i = 0.72 mm; □, Re_L = 150, y_i = 0.55 mm. (c) Aqueous sec.-octyl alcohol solution, $\mu_L = 9.0 \times 10^{-4}$ Nsec/m^2, Re_L = 4910, y_i = 0.85 mm.

1.2 m down from the liquid inlet section, is thought to depend on the liquid Reynolds number and its limiting value is estimated as 300 as a measure. Figure 12(c) shows a trend of the maximum height decreasing with a decrease of the surface tension.

Here, the relationship between the maximum height of liquid films and gas velocity will be examined. Figure 13 shows the increase in wave height of the films of $y_i \doteqdot 0.85$ mm at a position of $L = 1.75$ m for the gas velocity u. The ordinate represents the difference between y_{imax} and $y_{imax(0)}$, where $y_{imax(0)}$ denotes the maximum height of the liquid film at zero gas velocity. The data are widely scattered but suggest a trend of the wave height to increase approximately in proportion to $\rho_G u^2$. Figure 14 shows the values of the maximum height at $L = 1.75$ m near the liquid outlet plotted against the gas velocity. This figure is indicating that the wave height grows large with increasing gas velocity and flooding occurs when the maximum height reaches a certain limiting value. The solid points laying on extension of the curves represent the values corresponding to the flooding velocities. These flooding points obtained by such a method are summarized in figure 15.

The data in figure 15 are scattered because of the difficulties in measuring the maximum height arising from the generation of liquid droplets in the flow state close to flooding. Judging

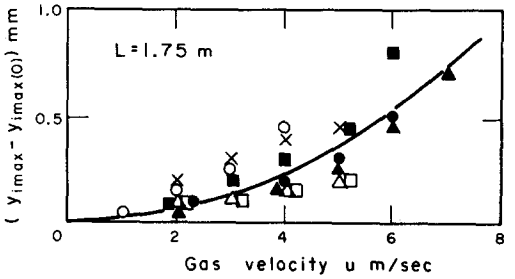

Figure 13. Growth of wave height by gas velocity ($D_i = 28.8$ mm, $L_d = 1.83$ m, $y_i \doteqdot 0.85$ mm).

	μ_L Nsec/m^2	σ N/m
○	9.0×10^{-4}	0.068
■	2.0×10^{-3}	0.056
▲	5.3×10^{-3}	0.053
●	9.5×10^{-3}	0.053
×	9.0×10^{-4}	0.055
△	9.0×10^{-4}	0.046
□	9.0×10^{-4}	0.037

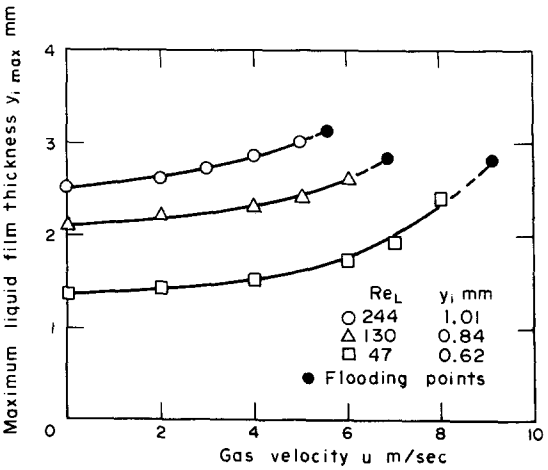

Figure 14. Maximum height of liquid film and gas velocity (aqueous glycerol solution, $D_i = 28.8$ mm, $L_d = 1.83$ m, $\mu_L = 9.5 \times 10^{-3}$ Nsec/m^2).

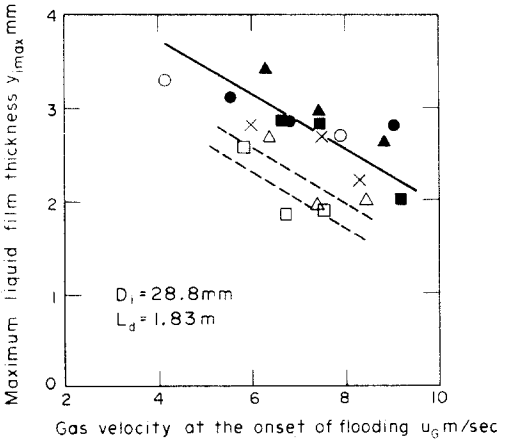

Figure 15. Maximum height of liquid film and flooding velocity. Keys are given in figure 13.

from the results in this figure, however, it is found that there is a relation between the flooding velocity and the maximum height of the liquid film at the flooding point, and that the limiting line representing this relation has a trend to fall with decreasing surface tension. From observation of the flow state described before, this limiting line is supposed to depend on the tube diameter and to have a trend to move to lower values of y_{imax} with a decrease of the tube diameter. A detailed discussion on the limiting line will be presented in the following paper, Part 2.

From the above description, it is suggested that the maximum height of liquid films at zero gas velocity plays an important part for determining the flooding velocity. The greater this value is, the lower is the flooding velocity. It can be reasonably understood from this fact that the tube floods more easily with increasing liquid flow rate and also with an increase of the tube length excepting the range of liquid Reynolds numbers less than about 300. Moreover, the effect of surface tension on flooding may be estimated as follows: if the surface tension is reduced, the maximum height of liquid films decreases as shown in figure 12 but the limiting line migrates to a lower position in figure 15. The two facts give opposite effects on flooding, then the flooding velocity takes its maximum value at a surface tension close to 5.0×10^{-2} N/m.

6. NONDIMENSIONAL REPRESENTATION OF FLOODING VELOCITY

Since the tube length affects the flooding condition in a complicated manner as discussed previously, nondimensional representation of flooding velocity is attempted for each tube length. As for the factors associated with flooding, the following four nondimensional groups are selected,

$$Fr \equiv [\rho_G(u_G + u_L)^2/\rho_L g y_i]^{1/2}, \qquad Re_L, \qquad (\rho_L g D_i^2/\sigma'), \qquad (\mu_G/\mu_L)$$

where $\rho_G(u_G + u_L)^2$ represents the kinetic energy of the gas phase based on the relative velocity between the gas and liquid, y_i the mean liquid film thickness, and σ' modified surface tension. The modified surface tension is defined taking into account the empirical fact that the flooding velocity takes its maximum value at $\sigma \doteqdot 0.05$ N/m as,

$$\sigma' = \sigma + 1.5|\sigma - 0.05| \text{ N/m}. \qquad [7]$$

Then, the Froude number will be expressed in terms of the other three groups as follows:

$$Fr = F\left[Re_L^{\,x} \cdot \left(\frac{\rho_L g D_i^2}{\sigma'}\right)^{y} \cdot \left(\frac{\mu_G}{\mu_L}\right)^{z}\right]. \qquad [8]$$

By using all the experimental data, the three constants in [8] were determined as $x = -1/3$, $y = 1/4$ and $z = 2/3$ respectively. Then,

$$Fr = F\left[Re_L^{-1/3} \cdot \left(\frac{\rho_L g D_i^2}{\sigma'}\right)^{1/4} \cdot \left(\frac{\mu_G}{\mu_L}\right)^{2/3}\right]. \quad [9]$$

Figures 16 and 17 show some of the results of flooding velocity which are rearranged in a form of [9]. From these results, the following empirical equations are derived for each tube

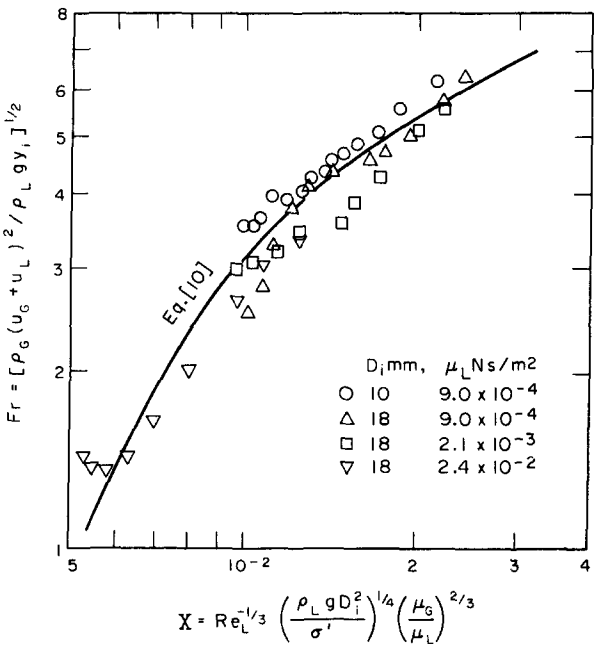

Figure 16. Flooding velocity correlation ($L_d = 0.5$ m).

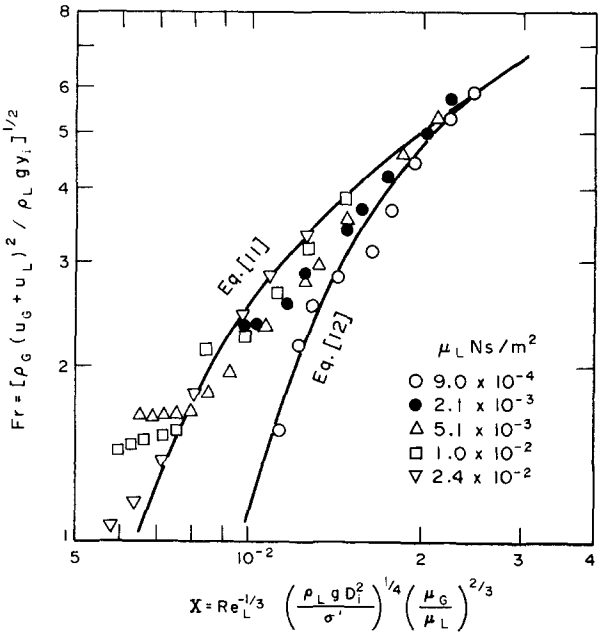

Figure 17. Flooding velocity correlation ($D_i = 18$ mm, $L_d = 1.5$ m).

length L_d, denoting the term in the bracket of the right hand side of [9] by X.

$L_d = 0.5$ m

$$Fr = 7.66 \log_{10} X + 18.37 \quad [10]$$

$L_d = 1.0$ m

$$Fr = 8.29 \log_{10} X + 19.18, \quad [11]$$

$L_d = 1.5$ m

$Re_L \leq 350$ or $\mu_L > 3 \times 10^{-3}$ Nsec/m^2: Equation [11]

$Re_L > 350$ or $\mu_L < 1 \times 10^{-3}$ Nsec/m^2:

$$Fr = 11.94 \log_{10} X + 25.0, \quad [12]$$

$L_d = 2.0$ m

$Re_L \leq 350$ or $\mu_L > 3 \times 10^{-3}$ Nsec/m^2: Equation [11]

$Re_L > 350$ or $\mu_L < 1 \times 10^{-3}$ Nsec/m^2:

$$Fr = 14.86 \log_{10} X + 29.7. \quad [13]$$

Figure 18 shows the correlation of the data obtained for various surface tensions and tube diameters in a tube length $L_d = 1.5$ m. The above equations will be compared here with the data which have been presented in papers. As is known generally, the flooding velocity is sensitive to the types of liquid inlet section. This suggests that the wave height of liquid film may be affected by the structure of liquid inlet section. Therefore, the data of Clift *et al.* (1966) and Hewitt *et al.* (1965) for a tube length $L_d = 1.83$ m were selected for this purpose, because both data were obtained by using similar liquid inlet sections to the present experiment. Figure 19

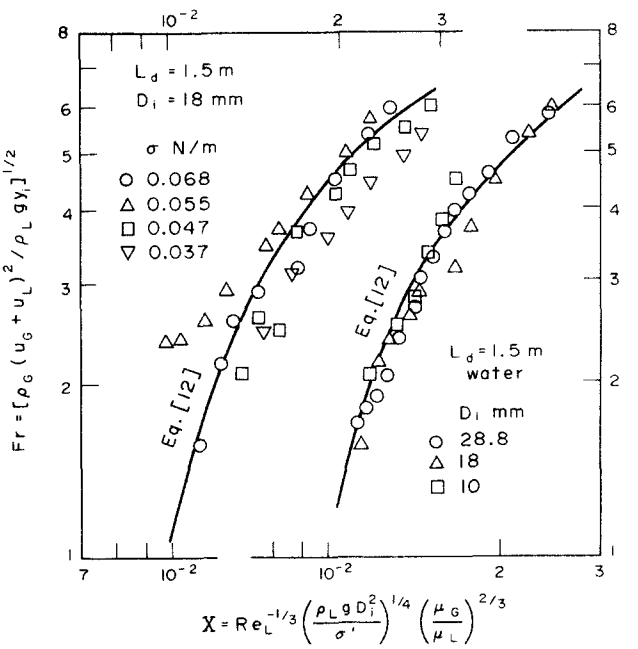

Figure 18. Flooding velocity correlation (surface tension and tube diameter).

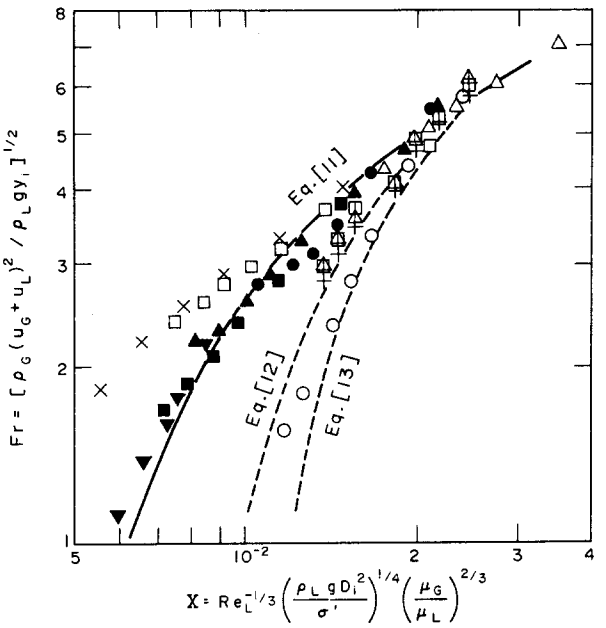

Figure 19. Comparison of the present correlations with the data of Clift & Hewitt (L_d = 1.83 m).

Present data D_i = 28.8 mm		Clift *et al.* D_i = 31.75 mm		Hewitt *et al.* D_i = 31.75 mm		
	μ_L (Nsec/m^2)		μ_L (Nsec/m^2)		μ_L (Nsec/m^2)	p (N/m^2)
○	9.0×10^{-4}	△	1.32×10^{-3}	⧋	1.32×10^{-3}	1.0×10^5
●	2.1×10^{-3}	□	1.04×10^{-2}	⧈	1.32×10^{-3}	1.4×10^5
▲	5.1×10^{-3}	×	8.25×10^{-2}	+	1.32×10^{-3}	2.75×10^5
■	1.0×10^{-2}					
▼	2.4×10^{-2}					

shows the comparison of these data with the above equations along with the present data for L_d = 1.83 m. Although some of the data of Clift for high viscous liquids deviate upwards from [11], the other data of Clift and the data of Hewitt obtained in a range of system pressures p from 1.0×10^5–2.75×10^5 N/m^2 are in good agreement with the present results.

7. CONCLUSIONS

An experiment was performed on the counter-current two-phase flow in vertical tubes. The flooding velocity was measured over a wide range of parameters and the maximum height of liquid films was examined. From the results, the following conclusions were obtained.

(1) A large amplitude wave which causes flooding is one of waves on the liquid film developed by the interaction between the waves and the gas stream, and is accompanied with a number of liquid droplets.

(2) The gas velocity at the onset of flooding increases with a decrease of liquid flow rate and an increase of tube diameter. Flooding velocity decreases with increasing tube length. For high viscous liquids, however, the effect of tube length on flooding is relatively small. The effect of surface tension is complicated and flooding velocity takes its maximum value at a surface tension close to 5.0×10^{-2} N/m.

(3) The greater the maximum height of the liquid film at zero gas flow rate is, the lower is the flooding velocity. The effects of liquid flow rate, tube length and surface tension on flooding can be explained by taking into account the characteristics of the maximum height of liquid films.

The nondimensional representation of flooding velocity was attempted on the basis of the measured results and [10]–[13] were presented.

REFERENCES

ADDISON, C. C. 1944 The properties of freshly formed surface. Part III. The mechanism of absorption, with particular reference to the sec.-octyl alcohol water system. *J. Chem. Soc.* 477–480.

ADDISON, C. C. 1945 The properties of freshly formed surface. Part IV. The influence of chain length and structure on the static and dynamic surface tensions of aqueous-alcohol solutions. *J. Chem. Soc.* 98–106.

CLIFT, R., PRITCHARD, C. L. & NEDDERMAN, R. M. 1966 The effect of viscosity on the flooding conditions in wetted wall columns. *Chem. Engng Sci.* **21**, 87–95.

GETINBUDAKLER, A. G. & JAMESON, G. J. 1969 The mechanism of flooding in vertical countercurrent two-phase flow. *J. Fluid Mech.* **22**, 1669–1680.

HEWITT, G. F. & HALL TAYLOR, N. S. 1970 *Annular Two-Phase Flow*, pp. 68–73. Pergamon Press, Oxford.

HEWITT, G. F., LACEY, P. M. C. & NICHOLIS, B. 1965 Transition in film flow in a vertical tube. *Proc. Symp. Two-Phase Flow*, Exeter. **2**, B401–430.

HEWITT, G. F. & WALLIS, G. B. 1963 Flooding and associated phenomena in falling film flow in a tube. AERE-R4022.

ISIGAI, S., NAKANISHI, S., KOIZUMI, T. & OYABU, Z. 1971 Hydrodynamics and heat transfer of vertical falling liquid films, Part 1. Classification of flow regimes. *Trans. Jap. Soc. Mech. Engrs* **37**, 1708–1715.

JONES, L. O. & WHITAKER, S. 1966 An experimental study of falling liquid films. *A.I.Ch.E. Jl* **12**, 525–529.

KAMEI, S., OISHI, J. & OKANE, T. 1954 Flooding in a wetted wall tower. *Chem. Engng (Jap.)* **18**, 364–368.

KUSUDA, H. & IMURA, H. 1974 Stability of a liquid film in a counter-current annular two-phase flow. *Trans. Jap. Soc. Mech. Engrs* **40**, 1082–1088.

LEVICH, V. 1962 *Physicochemical Hydrodynamics*, p. 620. Prentice-Hall, New York.

PORTALSKI, S. & CLEEG, A. J. 1972 An experimental study of wave inception on falling liquid films. *Chem. Engng Sci.* **27**, 1257–1265.

SHEARER, C. J. & DAVIDSON, J. F. 1965 The investigation of a standing wave due to gas blowing upwards over a liquid film; its relation to flooding in wetted-wall columns. *J. Fluid Mech.* **22**, 321–335.

SHIRES, G. L. & PICKERING, A. R. 1965 The flooding phenomenon in counter-current two-phase flow. *Proc. Symp. Two-Phase Flow*, Exeter. **2**, B501–538.

SHIROTSUKA, T., HONDA, N. & OHATA, Y. 1957 Wave motion on the falling film in a wetted-wall column of flat plate. *Chem. Engng (Jap.)* **21**, 702–707.

STAINTHORP, F. P. & BATT, R. S. W. 1965 The wave properties of falling liquid films with counter-current air flow. *Proc. Symp. Two-Phase Flow*, Exeter. **2**, B301–310.

UEDA, T. & TANAKA, T. 1973 Studies of liquid film flow in two-phase annular and annular-mist flow regions, Part I. Downflow in a vertical tube. *Trans. Jap. Soc. Mech. Engrs* **39**, 2842–2852. *Bull. Jap. Soc. Mech. Engrs* **17**, 614–624.

WALLIS, G. B. 1961 Flooding velocities for air and water in vertical tubes. AEEW-R123.

WALLIS, G. B. 1962 The influence of liquid viscosity on flooding in a vertical tube. G.E.Rep. No. 62 GL132.

WALLIS, G. B. 1969 *One Dimensional Two-Phase Flow*, pp. 336–346. McGraw–Hill, New York.